processes

MDPI

Article

Development and Evaluation of a Universal Seed Discharger for Precision Planting in Corn-Soybean Cropping System

Xinming Jiang [1], Jie Zhang [1], Shuyan Liu [2,3], Lili Fu [2,3] and Dongyan Huang [1,*]

[1] The College of Engineering and Technology, Jilin Agricultural University, Changchun 130118, China; jiangxinming@jlau.edu.cn (X.J.); zhangjie9804@163.com (J.Z.)
[2] Key Laboratory of Bionics Engineering, Ministry of Education, Jilin University, Changchun 130022, China; shuyan22@mails.jlu.edu.cn (S.L.); full23@mails.jlu.edu.cn (L.F.)
[3] College of Biological and Agricultural Engineering, Jilin University, Changchun 130022, China
* Correspondence: huangdy@jlu.edu.cn; Tel.: +86-136-107-12601

Abstract: Aiming at solving the problem of a wide variety of crop planting and addressing the concept of precision agriculture, a pneumatic universal seed-metering device suitable for corn and soybean was designed. According to the physical size of the above two crops crop planting, a seeding plate, a hole, and a guide tube were designed. The pressure distribution inside the seeding plate was studied, when the pressure, the diameter of the hole, and the rotation speed of the metering plate changed. Through the coupling simulation method of DEM and CFD, the effects of the air suction hole diameter, the air pressure intensity, and the seeding plate speed on the seeding performance were explored. The results showed that when the air suction hole diameter was 5.9 mm, the air pressure intensity was 3.5 kPa, and the seeding plate speed was 23.8 r/min, and the performance of corn seeding was the best, among which the seeding qualification index was 95.35%, the replay index was 1.45%, and the missed seeding index was 3.23%. When the air suction hole diameter was 6.1 mm, the air pressure intensity was 3.5 kPa, and the rotation speed of the seed plate was 24 r/min, the performance of soybean sowing was the best, in which the sowing qualification index was 95.76%, the reseeding index was 3.47%, and the missed sowing index was 0.77%. The bench verification test and the comparative test were carried out. The results showed that the seed-metering device had good seeding performance and could be applied to the general seeding operation of corn and soybean.

Keywords: pneumatic metering device; precision planting; DEM-CFD; bench test; universal

check for updates

Citation: Jiang, X.; Zhang, J.; Liu, S.; Fu, L.; Huang, D. Development and Evaluation of a Universal Seed Discharger for Precision Planting in Corn-Soybean Cropping System. *Processes* **2024**, *12*, 1595. https://doi.org/10.3390/pr12081595

Academic Editor: Hsin-Jang Shieh

Received: 18 June 2024
Revised: 24 July 2024
Accepted: 27 July 2024
Published: 30 July 2024

Copyright: © 2024 by the authors. Licensee MDPI, Basel, Switzerland. This article is an open access article distributed under the terms and conditions of the Creative Commons Attribution (CC BY) license (https://creativecommons.org/licenses/by/4.0/).

1. Introduction

According to the world's agricultural production statistics released by the Food and Agriculture Organization of the United Nations [1] and related literature reports [2,3], corn is the world's highest-yield grain, and soybean is the world's second-highest oil crop. Both play an important role in world food production security and sustainable agricultural development [4–6]. In the face of such a high yield, it is particularly important to integrate the concept of precision agriculture into the efficient sowing technology of corn and soybean. It can not only improve the sowing accuracy and efficiency of seeds [7–10], but also help to ensure that seeds are sown at the best depth and spacing, thereby improving crop yield and resource utilization efficiency. In the precision seeding operation, the seed-metering device is the key component to ensure the seeding performance on the seeder [11–14].

According to its working principle, the seed-metering device can be divided into two types: pneumatic and mechanical [15–18]. The mechanical seed-metering device is easy to damage seeds, and the precision is low [19,20]. A pneumatic metering device is suitable for high-speed precision seeding operation because of its small damage to seeds and high precision through airflow contact with seeds [21]. For pneumatic seeders, some scholars at home and abroad have also carried out related research. Kamran Shah et al. designed a variable-rate multi-crop air-suction seed-metering device, which realizes the sowing of corn

and soybean without replacing the seed-metering plate [22]. Wang Dongwei et al. designed an air-suction high-speed precision seed-metering device with drive-combined groove auxiliary attachment, which realizes the functions of disturbing, driving and auxiliary attachment and ensured the seeding performance during high-speed operation. The rationality of the structure design of the seeding plate was verified by theoretical modeling and analysis, and the key parameters were preliminarily determined [23]. Shi Shaobin et al. used the discrete element analysis software EDEM (2020, Altair Engineering Inc., Troy, MI, USA) to do simulation analysis and proved that the influence of the rotation speed of the metering device on the qualified index is greater than the groove angle and the influence of the suction hole spacing on the qualified index is small [24]. Liu Rui et al. designed a double-disturbance-assisted seed-filling high-speed air-suction seed-metering device. By increasing the seed-filling area, increasing the seed-filling time of the seed-metering plate, strengthening the population dispersion and reducing the adsorption pressure, the problem of poor operation caused by seed leakage and suction caused by high-speed operation of the corn air-suction seed-metering device was solved [25]. Through the analysis of the cleaning process, Ding Li constructed a parametric mathematical model of the cleaning mechanism of the air-suction seed-metering device and optimized the cleaning mechanism of the air-suction seed-metering device to reduce the problem of the high replay index of the corn air-suction seed-metering device [26]. Jia Honglei et al. analyzed the influence of key design parameters on population migration law through discrete element simulation design and theoretical modeling analysis and optimized the geometric structure parameters of key components to reduce the technical problems of air-suction high-speed precision seed-metering devices that are prone to a large number of missed seeding when the negative pressure plummets [27]. Karayel et al. determined the optimal vacuum pressure of a vacuum precision planter and established a mathematical model by using the physical characteristics of 1000-grain weight, sphericity, and density of seeds such as corn, soybean, and cotton [28]. Siyu He et al. designed an airflow cleaning mechanism that uses positive pressure airflow to blow out and reabsorb seeds, which improves the seeding accuracy [29]. The above scholars' research on pneumatic seed-metering devices is only for the same crop, and the sowing versatility between different crops is poor. It is usually necessary to replace the metering plate to achieve multi-category seed-sowing operations, and the operation efficiency is low [30–32]. At the same time, due to the demand for high-speed sowing and the complexity of field operations, the coefficient of variation of the seed spacing after sowing will be large. On the other hand, the pressure distribution of the internal flow field of the pneumatic seed-metering device is also more complex [33,34]. The influences of different operating parameters on its seeding performance need further study.

Based on the above problems, the authors took the representative maize and soybean varieties in Northeast China as the test objects, designed the key components of a universal seed-metering device for maize and soybean and studied the pressure distribution law inside the seed-metering device under different conditions. Through the DEM−CFD coupling simulation method, the optimal operating parameters of the seed-metering device suitable for the two crops were obtained. The rotation speed of the seed-metering disc was 23.8 r/min when sowing corn, and the rotation speed of the seed-metering disc was 24 r/min when sowing soybean. At this time, the seeding qualification index was not less than 95%, which provides a reference for the research of the universal seeder for maize and soybean.

2. Materials and Methods

2.1. Flow Chart of the Development and Evaluation Process of the Seed-Metering Device

In order to facilitate the understanding of the development and evaluation process of seed metering device, the flow chart of the process is made as shown in Figure 1.

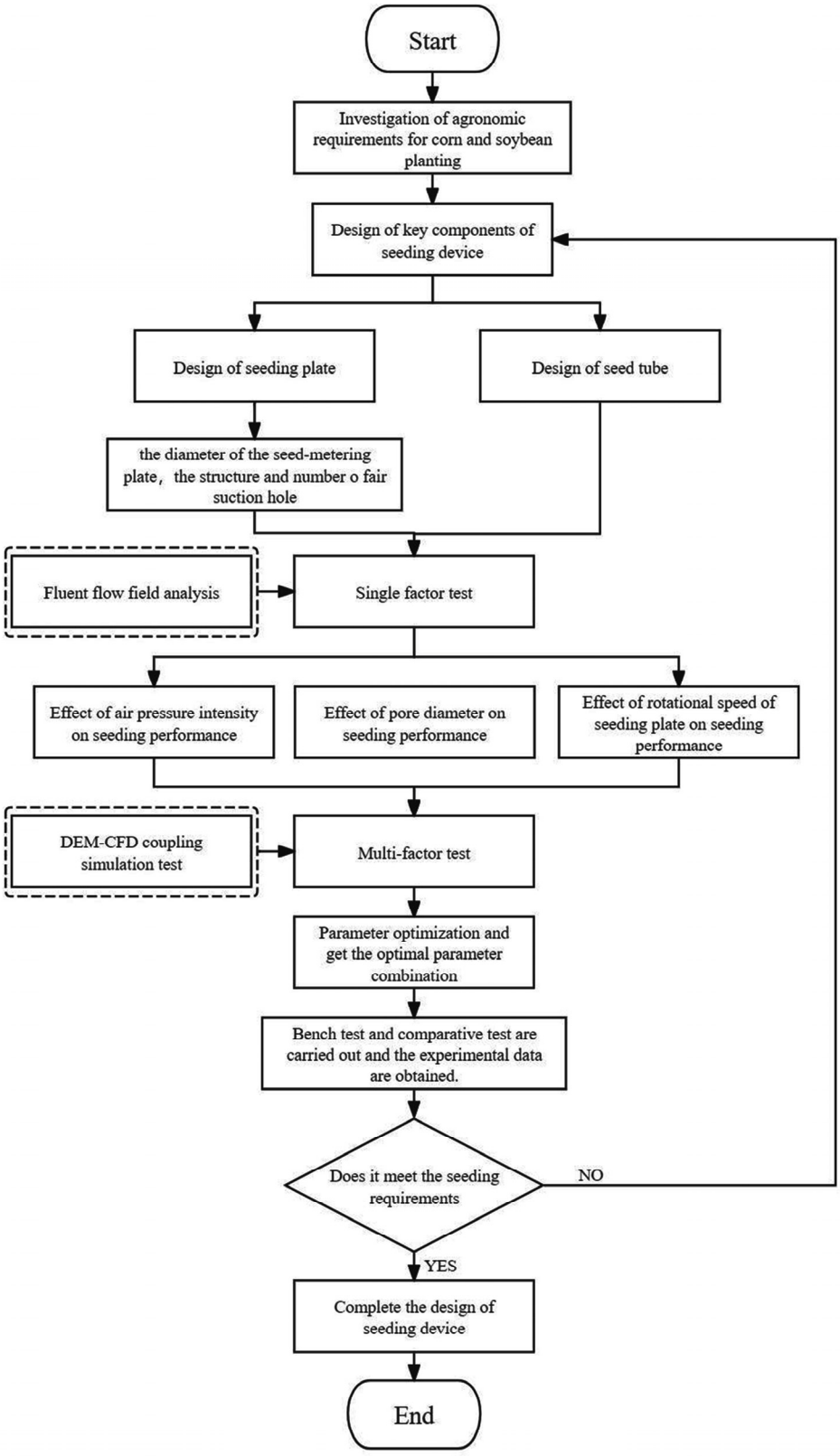

Figure 1. Flow chart.

2.2. The Structure and the Working Principle of the Seeding-Metering Device

The universal corn-soybean seed-metering device studied in this paper is mainly composed of a shell, an inlet pipe, a brush, a seed-metering plate, a transmission shaft, a seed-metering plate positioning seat, and a seed-metering device shell cover. The seed-

metering device shell and the brush are fastened by screws, and the seed-metering plate moves with the transmission shaft through the positioning seat. The seed-metering plate is designed with 24 holes, and the shell cover is composed of plastic materials, as shown in Figure 2.

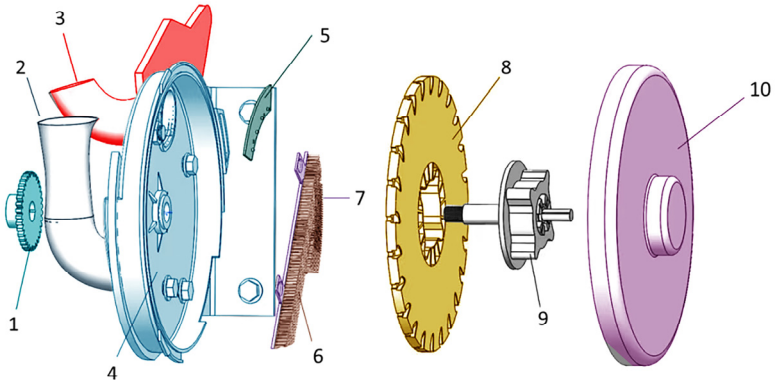

Figure 2. Schema diagram of the universal corn-soybean seed-metering device. 1. Transmission shaft; 2. inlet; 3. inlet; 4. shell; 5. brush one; 6. brush two; 7. brush three; 8. seeding plate; 9. positioning seat; 10. shell cover.

When the seed-metering device is running, the power system of the seeder drives the drive shaft to rotate, and the drive shaft drives the positioning seat, so that the metering plate moves. The airflow generated by the hydraulic fan enters the air chamber from the inlet, and the seeds in the seed box enter the air chamber from the inlet. Brush one is responsible for cleaning the seeds adsorbed outside the typed hole, brush two is responsible for isolating the wind pressure, and brush three is responsible for pressing the seeds into the typed hole. The seeding process is divided into four processes: filling, clearing, carrying, and seeding. The air flow presses the seeds into the typed hole and makes them rotate together with the seeding plate. After the brush, the seeds outside the typed hole are cleaned for a time to complete the clearing process. After the brush, the two or three seeds are pressed into the typed hole without air pressure to complete the carrying process. Finally, the seeds are carried to the seed-metering port, and the seeds fall to the surface in free fall to complete the seeding operation.

2.3. Design of the Seeding Plate

As the seed-carrying device of the seed-metering device, the seed-metering plate is the key structure of the seed-metering device. In order to design the seed-metering plate, the seed-metering typed hole, the diameter of the seed-metering plate, the number of typed holes, and the pores are mainly designed, to achieve the effect of universal seeding without replacing the seed-metering plate. The seed-metering holes are evenly distributed on the edge of the seed-metering plate, and the pores are distributed on the edge of each typed hole. The seed-metering plate is shown in Figure 3.

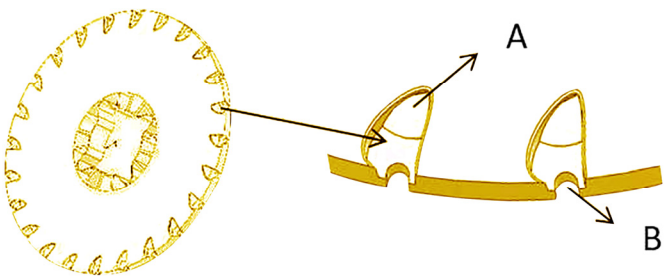

Figure 3. Schematic diagram of the seeding tray. (A) shaped hole; (B) stoma.

The diameter of the seed-metering plate and the number of the seed-metering holes are important parameters for the development of the seed-metering plate. The diameter of the seed-metering plate directly affects the size of each part of the seed-metering device, and the diameter of the seed-metering plate also affects the filling time of the seed. The smaller the diameter of the seed-metering plate, the shorter the filling time. The larger the diameter, the longer the filling time. The relationship between the diameter of the seeding plate D and the number of holes N is as follows:

$$S = \frac{2\pi}{N} \times \frac{D}{2}, \tag{1}$$

where S is the distance between two holes (mm); N is the number of holes in the seed discharge disk (one); D is the diameter of the seed discharge disk (mm).

The diameter D of the seeding plate needs to be designed according to the air chamber of the pneumatic metering device. The diameter of the seeding plate of the pneumatic metering device on the market is about 290 mm. According to the adjustment of the seeding chamber, considering the working performance of the seeding plate, the diameter D of the seeding plate is 280 mm, and the number of holes N is 24. Therefore, the distance S between the two types of holes is expressed as follows:

$$S = \frac{2\pi}{N} \times \frac{D}{2} = \frac{2\pi}{24} \times \frac{280}{2} \approx 36.63, \tag{2}$$

The overall structure of the seeding hole is that the back end is a trapezoidal opening, the front end is an arched surface, and the two sides of the wall are composed of a semi-circular hole and an increasing depth from the front end to the back end. The edge of the seeding plate hole is designed with a hole to form a pressure difference between the inside and the outside, so that the seed is firmly attached to the hole. The seeding plate hole is shown in Figure 4.

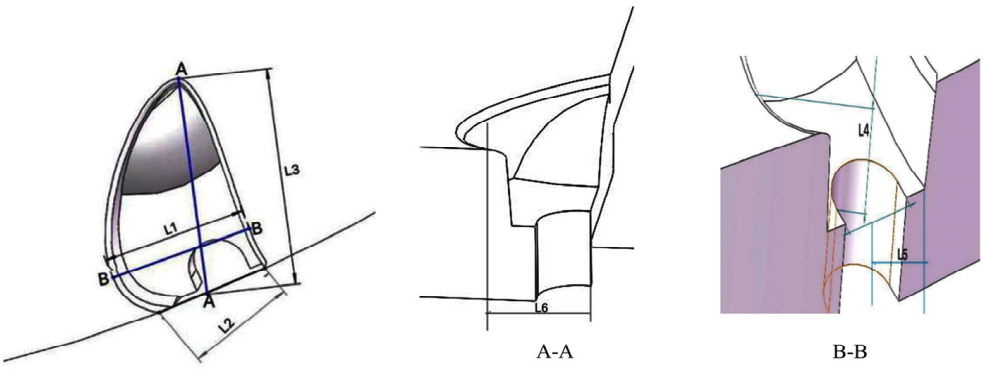

Figure 4. Seeding plate hole schematic diagram. (**a**) Typed hole structure diagram; (**b**) A-A section diagram; (**c**) B-B section diagram.

Combining the data obtained from the analysis of the physical properties of corn and soybean, the maximum equivalent diameter of corn is D_1, and the minimum equivalent diameter of soybean is D_2. Combining the above schematic diagram (Figure 4) of the type of holes, the following geometric relationships can be derived:

$$L_2 < L_1, \tag{3}$$

$$D_1 < 2D_2, \tag{4}$$

While ensuring that the typed hole of the seeding plate can be smoothly seeded, the typed hole can maintain a good seed-carrying state. When the seed enters the typed hole, it

is necessary to ensure that there are not two or more seeds at the same time to ensure the seeding accuracy, so the following geometric relationship needs to be met:

$$D_1 < L_2 < 2D_1, \tag{5}$$

The side wall of the seeding plate hole is a wall surface with a gradual increase in depth from the front end to the back end. It has an auxiliary supporting and fixing effect on the seed to prevent the seed from falling off when it enters the hole, that is, half of the equivalent radius of the seed in the hole is lower than the height of the hole wall. It is necessary to meet the following geometric relationship:

$$L_4 > \frac{D_1}{2}, \tag{6}$$

To make the front arch surface of the hole and the side wall of the-seed metering device have the effect of auxiliary support and fixation for the seed, the distance L_5 from the center of the hole to the side wall and the distance L_6 from the front arch surface need to meet several geometric relationships:

$$L_5 > \frac{D_2}{2}, \tag{7}$$

$$L_6 \geq \frac{D_1}{2}, \tag{8}$$

2.4. Design of the Seed Tube

The process of seeding can be divided into two processes. the first process is that the seed is discharged through the seed-metering device, impacts on the straight part of the seed guide tube and slides down against the back wall of the straight part of the tube after experiencing a few bounces; the second part is that the seed slides down through the straight part of the tube, enters into the curved part of the tube and is finally discharged from the outlet of the tube, wherein the curved part of the tube is based on the Archimedean solenoid to carry out the design of the tube. The guide tube is shown in Figure 5.

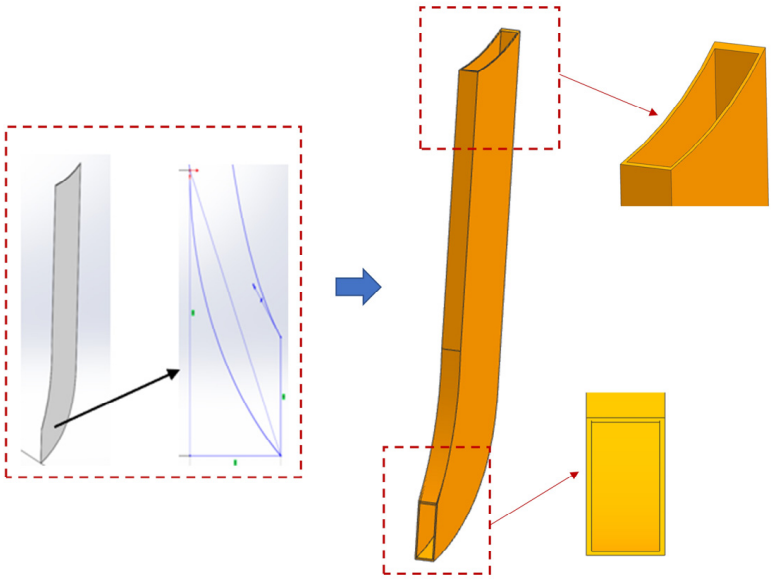

Figure 5. Structure diagram of the seed catheter.

The airflow enters the inside of the seed-metering device, so that the whole air chamber is in a positive pressure environment. The seed rotates with the seed-metering plate, and the seed is pressed into the hole of the seed-metering plate by the pressure adhesion force

generated by the airflow. When the seed reaches the seeding area, the seeding process is realized by the action of its gravity. Because there are stomata on the hole of the seed-metering plate, the pressure difference is generated here, and the airflow presses the seed into the hole. Therefore, the size of the pore diameter must have an impact on the airflow field. Because the stomata are located on the seed-metering plate, the rotation of the seed-metering plate will inevitably cause a change of the air pressure in the air chamber of the seed metering device, especially at the moment when the seed is just pressed into the hole by the airflow. The positive pressure intensity has a direct impact on the flow field.

3. Coupled Simulation Test

3.1. Single-Factor Test

In this paper, the seeding plate was designed based on the pneumatic metering device, because the internal pressure distribution of the metering device affected the seeding performance of the metering device. Several reasons affect the internal pressure distribution of the metering device. First, the pressure intensity directly determined the pressure inside the metering device, which in turn affected the internal pressure distribution of the metering device. Second, the size of the hole diameter of the seeding plate affected the airflow velocity around the hole. The smaller the hole diameter, the greater the airflow velocity around it. Then, the pressure distribution was changed. Third, the rotational speed of the seeding plate affected the internal pressure distribution of the metering device. The internal airflow velocity of the metering device decreased with the increase of the rotational speed, which led to a change in the internal pressure of the metering device. Therefore, the single-factor simulation test was carried out by EDEM (2020, Altair Engineering Inc., Troy, MI, USA) and FLUENT (2020 R2, ANSYS Inc., Canonsburg, PA, USA) software coupling around the air pressure intensity, the air suction hole diameter, and the seeding disc speed, and the influence of various factors on the seeding quality of the seed-metering device was explored.

3.1.1. Effect of the Air Pressure Intensity on the Seeding Performance

The diameter of the seeding plate was set to 5.5 mm, the rotation speed of the seed-metering device was set to 24 r/min, and the air pressure intensity was set to 2 kPa, 3 kPa, 4 kPa, 5 kPa, and 6 kPa. The corresponding velocity vector distribution maps and the pressure distribution cloud maps of the seeding plate under different air pressure intensities are shown in Figures 6 and 7.

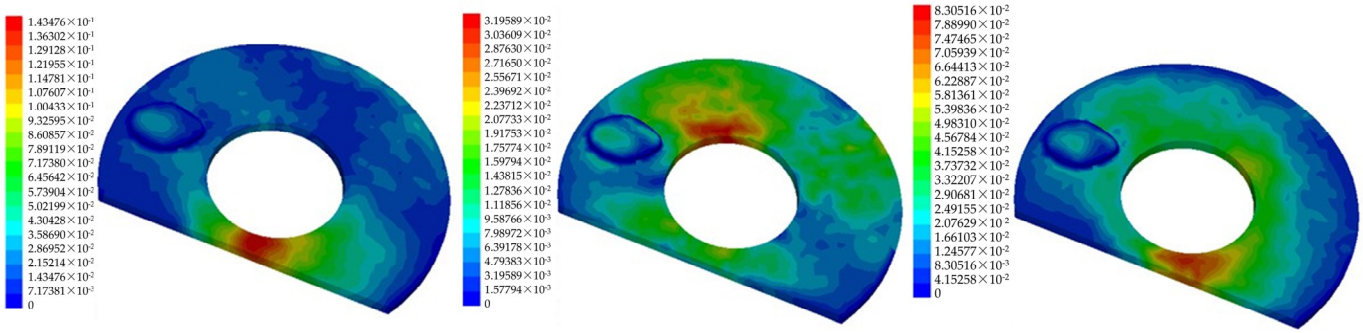

(**a**) (**b**) (**c**)

Figure 6. Velocity vector distributions at different air pressure intensities: (**a**) 2 kPa; (**b**) 4 kPa; (**c**) 6 kPa.

From the velocity vector distribution diagrams and the pressure distribution cloud diagrams, it can be seen that in the area near the center of the transmission shaft, the airflow velocity was significantly larger than in the surrounding area, and the maximum airflow velocity was near the axis and the position of the pressing brush. As the value of air pressure continued to increase, the area of low air pressure further shifted to the entrance,

the area of the maximum distribution was also close to the area of the pressing brush, and the area was smaller.

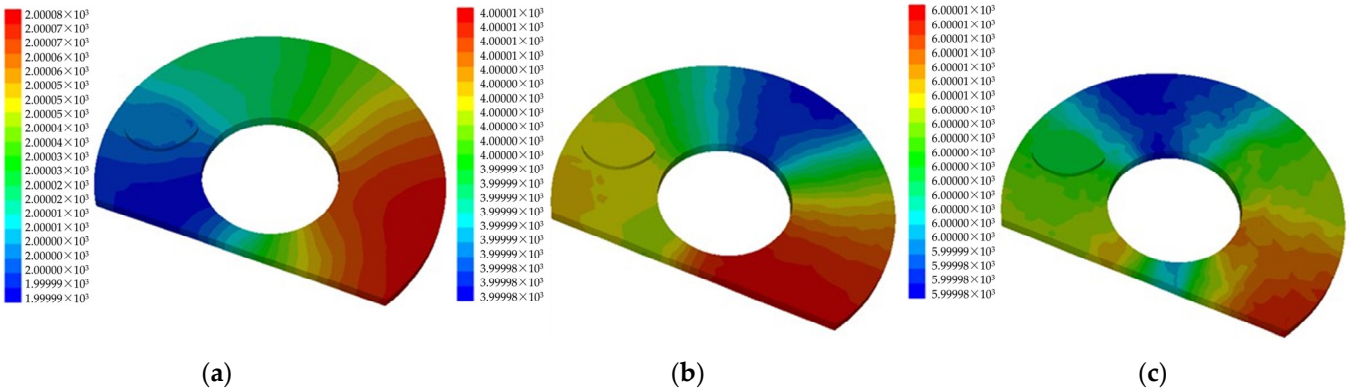

(**a**) (**b**) (**c**)

Figure 7. Pressure distribution cloud charts at different air pressure intensities: (**a**) 2 kPa; (**b**) 4 kPa; (**c**) 6 kPa.

The results of the coupling simulation test of sowing corn and soybean under different air pressures are shown in Figure 8.

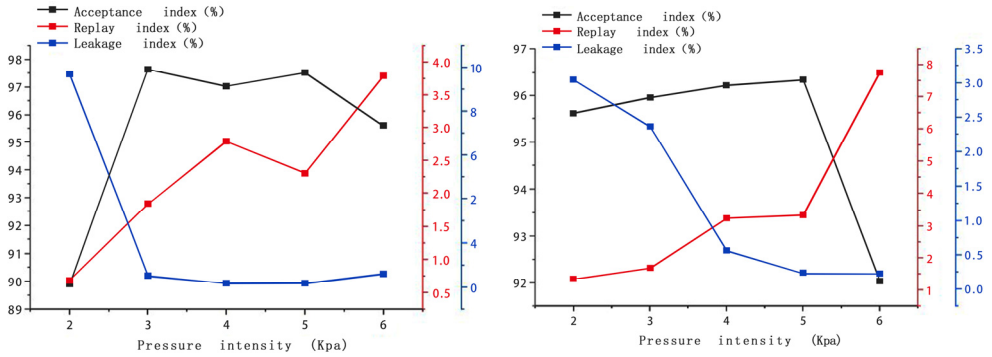

(**a**) (**b**)

Figure 8. Effects of the air pressure intensity on the performance of the seed-metering device: (**a**) corn; (**b**) soybean.

The single-factor experiment showed that with the increase of the air pressure intensity, the qualified indexes of corn and soybean increased first and then decreased. When the air pressure was 2 kPa, the qualified index of corn was much smaller than that of soybean. The reason was that the diameter and weight of soybean seeds were small. Even if the air pressure was small, the soybean seeds could be well covered in the typed hole while the weight of corn seeds was large, and it was not easy to be covered in the typed hole when the air pressure was small, resulting in a high missing index. When the air pressure increased from 5 kPa to 6 kPa, the qualified index of soybean decreased from 96.33% to 92.03%. The reason was that with the increase in air pressure, too many soybean seeds were accumulated in the typed hole and the reseeding index was too high.

3.1.2. Effect of the Pore Diameter on the Seeding Performance

The rotation speed of the seed plate was set to 24 r/min, the air pressure intensity was set to 4 kPa, and the air suction hole diameter was set to 5 mm, 5.5 mm, 6 mm, and 6.5 mm. The velocity vector distribution maps and pressure distribution cloud maps of the seed plate under different air suction hole diameters are shown in Figures 9 and 10.

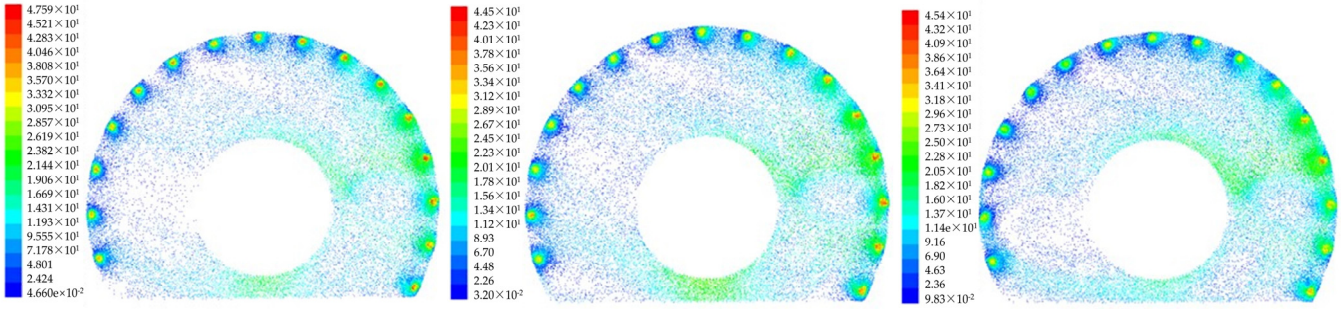

(**a**) (**b**) (**c**)

Figure 9. Velocity vector distributions with different air suction hole diameters: (**a**) 5.5 mm; (**b**) 6 mm; (**c**) 6.5 mm.

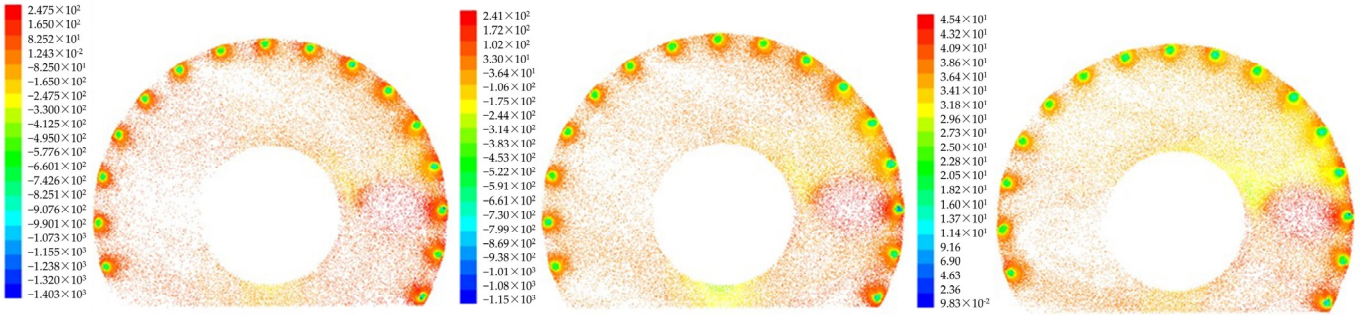

(**a**) (**b**) (**c**)

Figure 10. Pressure distribution cloud charts with different air suction hole diameters: (**a**) 5.5 mm; (**b**) 6 mm; (**c**) 6.5 mm.

It can be seen from the figures that the flow fields under different pore diameters were not much different and the airflow velocities through the hole were not very different. The airflow velocity was the maximum at the center of the hole. The average airflow velocity under three different air suction hole diameters was 44.5−47.6 m/s. The seed-metering device can maintain a high pressure when working. The pressure was mainly distributed near the hole, which was hemispherically distributed, and the pressure at the center of the hole was the smallest, but the pressure gradient was not high.

The results of the coupling simulation test of sowing corn and soybean under different air suction hole diameters are shown in Figure 11.

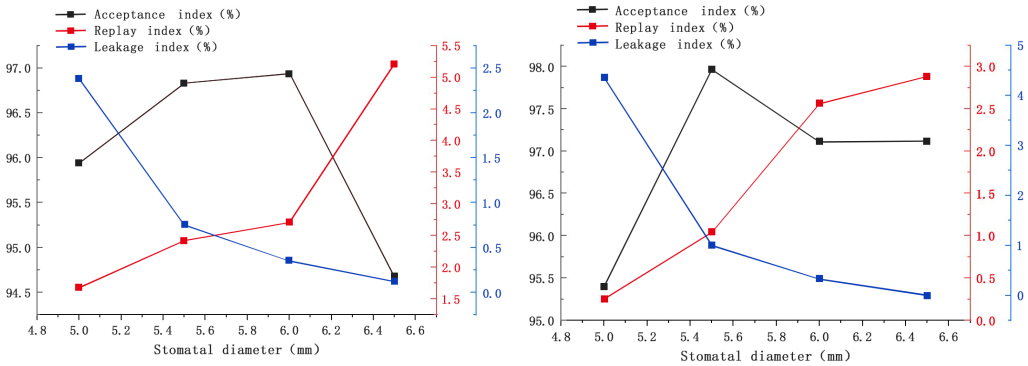

(**a**) (**b**)

Figure 11. Effects of the air hole diameter on the performance of the seed-metering device: (**a**) corn; (**b**) soybeans.

The single-factor experiment showed that with the increase of the air suction hole diameter, the qualified indexes of the two crops increased first and then decreased, and the leakage indexes decreased and then tended to be stable with the increase of the air suction hole diameter. The replay index gradually increased with the increase of the air suction hole diameter. When the pore diameter became larger, the area of the pores covered by the air pressure also increased, and it was easy to press two or more seeds into the typed hole, resulting in reseeding, which in turn affected the sowing quality.

3.1.3. Effect of the Rotational Speed of the Seeding Plate on the Seeding Performance

The diameter of the seeding plate was set to 5.5 mm, the air pressure intensity was set to 4 kPa, and the speed of the seed-metering device was set to 16 r/min, 20 r/min, 24 r/min, 28 r/min, and 32 r/min. The velocity vector distribution maps and the pressure distribution cloud maps of the seeding plate under different seeding plate speeds are shown in Figures 12 and 13.

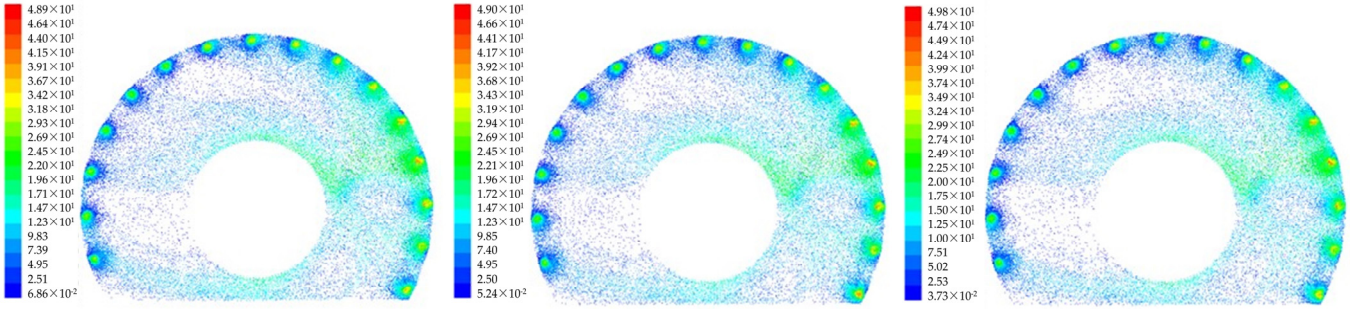

(**a**) (**b**) (**c**)

Figure 12. Velocity vector distributions at different speeds of the seed-metering device: (**a**) 20 r/min; (**b**) 24 r/min; (**c**) 28 r/min.

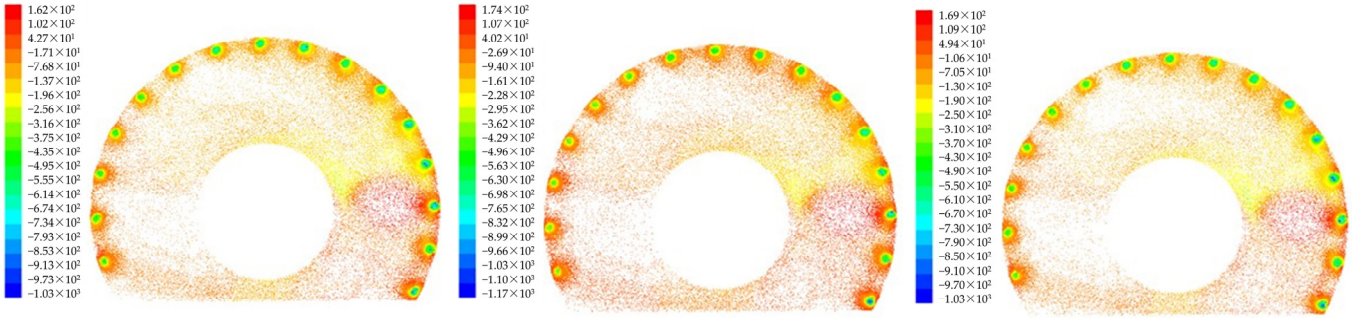

(**a**) (**b**) (**c**)

Figure 13. Pressure distribution cloud diagrams at different speeds of the seed-metering device: (**a**) 20 r/min; (**b**) 24 r/min; (**c**) 28 r/min.

It can be seen from the figures that when the air pressure and the pore diameter were constant, the flow field in the center of the hole had the best passing ability under the condition of a low rotation speed, and the airflow velocity decreased with the increase of the rotation speed, which led to the increase of the pressure in the air chamber of the metering device, but with the increase of the rotation speed, the gas flow field around the pore did not change much.

It can be seen from Figures 9–13 that when the air pressure intensity and the diameter of the air suction hole were constant, the flow field passing through the center of the air suction hole was the best when the rotation speed of the seeding plate was low, and the airflow velocity decreased with the increase of the rotation speed of the seeding plate,

which led to the increase of the pressure in the air chamber of the seeding device. However, with the increase of the rotation speed of the seeding plate, the gas flow field around the stomata did not change much.

The results of the coupling simulation test of sowing corn and soybean under different seeding plate speeds are shown in Figure 14.

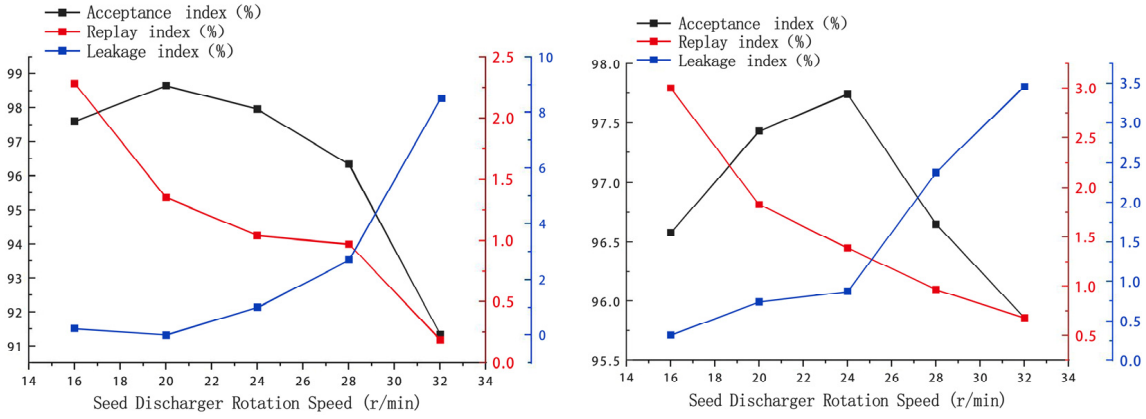

Figure 14. Effects of the rotation speed of the seed-metering disc on the seeding performance of the seed-metering device: (**a**) corn; (**b**) soybean.

The single-factor experiment showed that with the increase of the rotation speed of the seeding plate, the qualified indexes of the two seeds of corn and soybean increased first and then decreased. The reason is that when the rotation speed was low, the excess seeds were pressed into the hole and the reseeding index was too high. When the rotation speed of the seeding plate reached 20−24 r/min, the qualified indexes of the two seeds were the highest. When the rotation speed continued to increase, the qualified index decreased. The reason is that when the rotation speed of the seeding plate increased, the seeds were not pressed into the hole and caused missed sowing.

Through the single-factor tests on the air pressure intensity, the rotation speed of the seed plate, and the pore diameter, it was found that when one of the factors was changed, it affected the flow field in the seed-metering device, and when the flow field in the seed-metering device was changed, the qualified indexes of sowing corn and soybean were changed, and the sowing quality was reduced.

3.2. Multi-Factor Test

3.2.1. Establishment of the Seed Model

The corn seed model was established by using the filling function of non-spherical particles in EDEM software, as shown in Figure 15a. Because of the high sphericity of soybean seeds, a single spherical particle was used for modeling, as shown in Figure 15b.

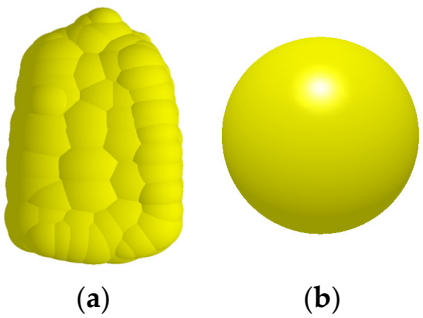

Figure 15. Seed model. (**a**) Corn seed model; (**b**) Soybean seed model.

3.2.2. Simulation Process

Through the single-factor experiments of sowing corn and soybean on air pressure intensity, the rotation speed of the seeding plate, and the air suction hole diameter, it was found that when one of the factors changed, it affected the flow field in the metering device, and when the flow field in the metering device changed, the qualified index of sowing corn and soybean changed, thus reducing the sowing quality. Design-Expert was used to design a three-factor and five-level experiment with the qualified index, the reseeding index, and the missing index as evaluation indexes. The simulation experiment was carried out by EDEM-FLUENT coupling to explore the interaction of these three experimental factors on sowing performance. Before the simulation, grid independence was also studied. In the process of grid independence verification, three kinds of grids, i.e., coarse grid, medium grid and fine grid, were used to simulate the air pressure intensity inside the metering device, and the corresponding test was compared with the actual test. Keeping the other conditions the same, when the air pressure intensity inside the seed-metering device was simulated by three kinds of grids, the conclusion was that the air pressure intensity changed greatly when the coarse grid and the medium grid were used separately, and the air pressure intensity changed little when the medium grid and the fine grid were used separately. The results showed that both the medium grid and the fine grid can accurately predict the seeding performance of the seed-metering device. At the same time, the results also showed that increasing the number of grids on the basis of the medium grid had little effect on the calculation results. Considering the calculation efficiency, the medium grid was selected for simulation calculation.

The filling and seeding processes of maize and soybean are shown in Figures 16 and 17, respectively.

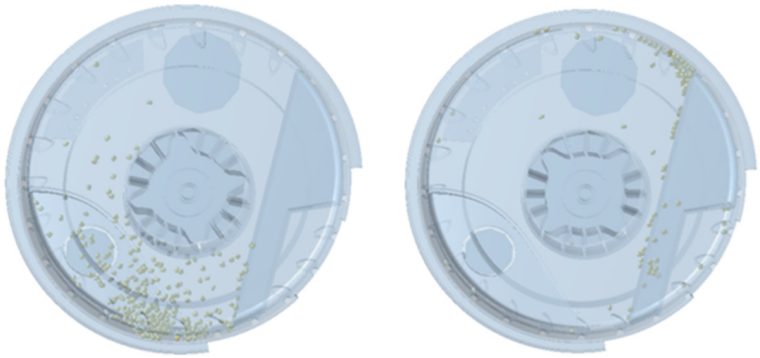

(**a**) (**b**)

Figure 16. Schema of the maize-sowing process. (**a**) Corn seed filling; (**b**) corn seeding.

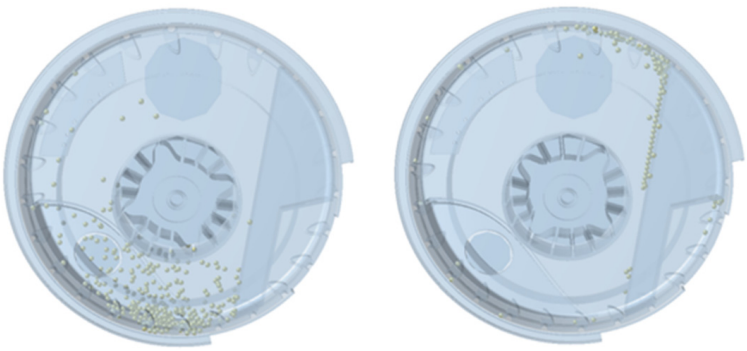

(**a**) (**b**)

Figure 17. Schema of the soybean-sowing process. (**a**) Soybean seed filling; (**b**) soybean seeding.

3.2.3. Test Results

The coupling simulation test was carried out according to the designed test scheme. The test scheme and test results of corn and soybean are shown in Tables 1 and 2, respectively.

Table 1. Corn test results.

Number	Factor			Index		
	Air Suction Hole Diameter (mm)	Barometric Strength (kPa)	Seed Discharge Disk Speed (r/min)	Acceptance Index (%)	Replay Index (%)	Leakage Index (%)
1	5.5	3	20	95.12	1.37	3.51
2	5.8	6	22	95.19	3.55	1.26
3	5.5	5	24	94.75	3.34	1.91
4	5.8	4	22	95.65	2.27	2.08
5	5.8	4	22	95.32	1.98	2.7
6	5.8	4	22	95.66	2.21	2.13
7	5.8	2	22	94.74	1.47	3.79
8	6.1	5	20	95.03	3.4	1.57
9	6.4	4	22	94.52	1.75	3.73
10	5.8	4	22	95.71	2.32	1.97
11	5.8	4	22	95.59	1.48	2.93
12	5.8	4	26	95.35	2.71	1.94
13	6.1	5	24	94.38	3.15	2.47
14	5.5	3	24	94.97	1.47	3.56
15	6.1	3	24	94.72	2.05	2.23
16	5.8	4	18	95.42	2.17	2.41
17	5.8	4	22	95.61	1.92	2.47
18	6.1	3	20	94.77	2.77	2.46
19	5.2	4	22	94.68	1.46	3.86
20	5.5	5	20	95.55	2.74	1.71

Table 2. Soybean test results.

Number	Factor			Index		
	Air Suction Hole Diameter (mm)	Barometric Strength (kPa)	Seed Discharge Disk Speed (r/min)	Acceptance Index (%)	Replay Index (%)	Leakage Index (%)
1	5.2	4	22	95.31	3.47	1.22
2	5.8	4	22	95.52	3.26	1.22
3	5.5	5	20	95.77	3.47	0.76
4	5.8	4	18	95.62	3.51	0.87
5	5.5	5	24	95.27	3.13	1.6
6	5.8	6	22	94.72	3.53	1.75
7	6.1	5	20	94.87	3.64	1.49
8	5.8	4	22	95.45	3.11	1.44
9	6.1	5	24	94.67	3.47	1.86
10	5.5	3	24	94.72	3.13	2.15
11	5.8	4	22	95.71	3.39	0.9
12	6.1	3	20	94.64	3.14	2.22
13	5.8	4	22	95.63	3.12	1.25
14	5.8	2	22	94.63	2.95	2.42
15	6.4	4	22	94.79	3.43	1.78
16	5.8	4	22	95.57	3.35	1.08
17	5.8	4	22	95.37	3.17	1.46
18	5.5	3	20	94.93	3.45	1.62
19	6.1	3	24	94.57	2.77	2.66
20	5.8	4	26	94.91	3.11	1.98

4. Results and Discussion

4.1. Test Results and the Establishment of the Regression Model

According to the test results of corn and soybean, the variance analysis was carried out, and the analysis results are shown in Tables 3 and 4. From the tables, it can be seen that the *p*-values of the qualified index, the reseeding index, and the missed seeding index of maize and soybean seeds were all less than 0.05, and the model was significant. Through the significance test, the model was effective. In the corn test of the qualification index model, X_1, X_3, X_2X_3, ${X_1}^2$, and ${X_2}^2$ had significant effects on the model, and the other items had no significant effect on the model. In the replay index model, X_1, X_2, ${X_2}^2$ and ${X_3}^2$ had significant effects on the model, while other factors have no significant effects on the model. The missed sowing index model, X_2 and ${X_1}^2$ had significant effects on the model, and the other effects were not significant. In the soybean test of the conformity index model, X_1, X_2, X_3, X_1X_2, ${X_1}^2$, ${X_2}^2$ and ${X_3}^2$ had significant effects on the model, and the other effects were not significant. In the replay index model, X_2, X_3, X_1X_2, and ${X_1}^2$ had significant effects on the model, and the rest of the effects were not significant. In the leakage index model, X_1, X_2, X_3, and ${X_2}^2$ shadowed the model.

$$\left\{\begin{array}{l} A = 95.59 + 0.1288X_1 + 0.1294X_3 - 0.1563X_2X_3 - 0.3575{X_1}^2 - 0.2284{X_2}^2 \\ D = 2.02 - 0.2151X_1 - 0.6201X_2 + 0.2418{X_2}^2 + 0.2171{X_3}^2 \\ M = 2.39 + 0.6188X_2 + 0.4092{X_1}^2 \end{array}\right\}, \quad (9)$$

$$\left\{\begin{array}{l} A = 95.54 + 0.2601X_1 - 0.1370X_2 + 0.1592X_3 - 0.1325X_1X_2 - 0.1809{X_1}^2 \\ -0.3135{X_2}^2 - 0.1049{X_3}^2 \\ D = 3.24 - 0.1608X_2 + 0.1371X_3 + 0.1475X_1X_2 + 0.0630{X_1}^2 \\ M = 1.22 - 0.2227X_1 + 0.2978X_2 - 0.2963X_3 + 0.3247{X_2}^2 \end{array}\right\}, \quad (10)$$

Table 3. Maize variance analysis.

Source	Qualified Index A/%				Replay Index D/%				Missing Index M/%			
	SS	**df**	**F**	***p*-Value ***	**SS**	**df**	**F**	***p*-Value ***	**SS**	**df**	**F**	***p*-Value ***
Model	3.12	9	10.70	0.0005 **	8.26	9	7.98	0.0016 **	9.74	9	5.43	0.0071 **
X_1	0.2266	1	6.99	0.0245 *	0.6319	1	5.49	0.0411 *	0.3476	1	1.74	0.2163
X_2	0.0576	1	1.78	0.2120	5.25	1	45.66	0.0001 **	5.11	1	25.62	0.0005 **
X_3	0.2288	1	7.06	0.0240 *	0.0298	1	0.2593	0.6217	0.0012	1	0.0062	0.9390
X_1X_2	0.0105	1	0.3245	0.5815	0.2850	1	2.48	0.1465	0.9800	1	4.91	0.0510
X_1X_3	0.0078	1	0.2412	0.6340	0.3486	1	3.03	0.1123	0.0221	1	0.1105	0.7464
X_2X_3	0.1953	1	6.03	0.0339 *	0.1176	1	1.02	0.3357	0.2048	1	1.03	0.3348
${X_1}^2$	1.84	1	56.84	0.0001 **	0.0880	1	0.7648	0.4024	2.41	1	12.10	0.0059 **
${X_2}^2$	0.7519	1	23.21	0.0007 **	0.8429	1	7.33	0.0220 *	0.0228	1	0.1145	0.7421
${X_3}^2$	0.0921	1	2.84	0.1227	0.6792	1	5.91	0.0354 *	0.3855	1	1.93	0.1947
Residual	0.3239	10			1.15	10			1.99	10		
Lack of fit	0.2277	5	2.37	0.1830	0.6589	5	1.34	0.3776	1.26	5	1.72	0.2832
Error	0.0962	5			0.4912	5			0.7336	5		
Total	3.44	19			9.41	19			11.74	19		

Note: * indicates significant effect ($0.01 < p < 0.05$), ** indicates extremely significant effect ($p < 0.01$).

To explore the influences of the interaction of various factors on the test index, the Design-Expert software (8.0.6, Stat-Ease Inc., Minneapolis, MN, USA) was used to process the test data of corn and soybean, and the response surface was drawn. The qualified index was the key index of the seed-metering device and an important basis for measuring whether the seed-metering device could complete the sowing operation. Therefore, the response surface of the qualified index was drawn according to the regression results of corn and soybean seeds, and the influences of the test factors on the qualified index were

analyzed. The influences of corn and soybean test indexes on the qualified index are shown in Figures 18 and 19, respectively.

Table 4. Soybean variance analysis table.

Source	Qualified Index A/%				Replay Index D/%				Missing Index M/%			
	SS	df	F	*p*-Value *	SS	df	F	*p*-Value *	SS	df	F	*p*-Value *
Model	3.17	9	14.01	0.0001 **	0.8562	9	10.02	0.0006 **	4.80	9	12.92	0.0002 **
X_1	0.5800	1	23.10	0.0007 **	0.0038	1	0.3983	0.5421	0.6775	1	16.41	0.0023 **
X_2	0.2564	1	10.21	0.0096 **	0.3529	1	37.16	0.0001 **	1.21	1	29.33	0.0003 **
X_3	0.3461	1	13.78	0.0040 **	0.2568	1	27.04	0.0004 **	1.20	1	29.05	0.0003 **
X_1X_2	0.1404	1	5.59	0.0396 *	0.1740	1	19.33	0.0016 **	0.0018	1	0.0436	0.8388
X_1X_3	0.0242	1	0.9637	0.3494	0.0018	1	0.1895	0.6725	0.0392	1	0.9495	0.3528
X_2X_3	0.0220	1	0.8781	0.3708	0.0040	1	0.4265	0.5285	0.0072	1	0.1744	0.6851
X_1^2	0.4717	1	18.78	0.0015 **	0.0572	1	6.03	0.0340 *	0.2004	1	4.85	0.0522
X_2^2	1.42	1	56.40	0.0001 **	0.0018	1	0.1915	0.6710	1.52	1	36.81	0.0001 **
X_3^2	0.1586	1	6.32	0.0307 *	0.0026	1	0.2772	0.6100	0.1204	1	2.92	0.1185
Residual	0.2511	10			0.0950	10			0.4128	10		
Lack of fit	0.1758	5	2.34	0.1867	0.0240	5	0.3388	0.8700	0.1841	5	0.8048	0.5913
Error	0.0753	5			0.0709	5			0.2288	5		
Total	3.42	19			0.9512	19			5.21	19		

Note: * indicates significant effect ($0.01 < p < 0.05$), ** indicates extremely significant effect ($p < 0.01$).

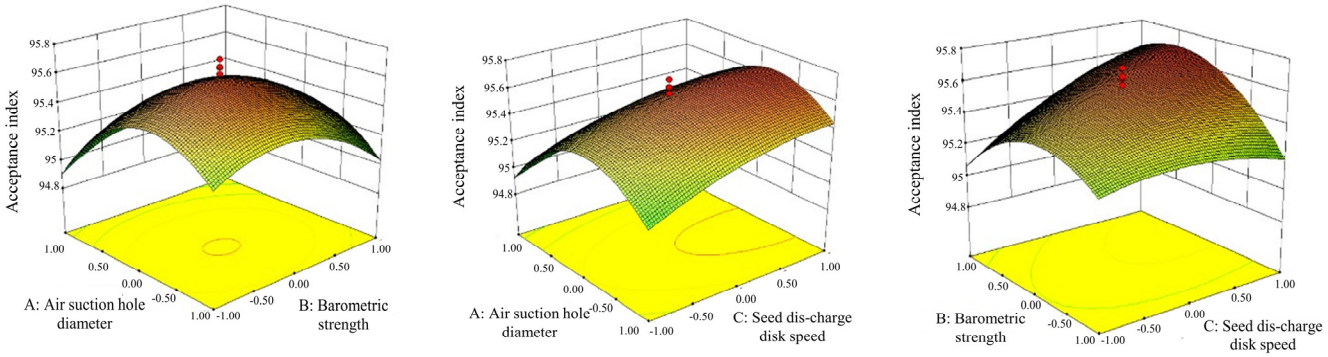

(a) **(b)** **(c)**

Figure 18. Effects of corn test factors on the qualifying index. (**a**) $X_3 = 0$; (**b**) $X_2 = 0$; (**c**) $X_1 = 0$.

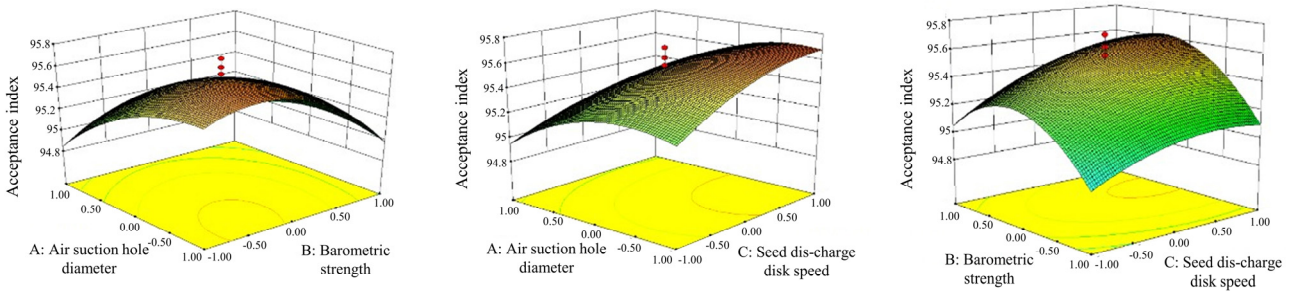

(a) **(b)** **(c)**

Figure 19. Effects of soybean test factors on the conformity index. (**a**) $X_3 = 0$; (**b**) $X_2 = 0$; (**c**) $X_1 = 0$.

It can be seen from the influences of the interaction factors of corn on the qualified index that when C was at the central level (22 r/min), the qualified index increased first and then decreased with the increase of B, and with the increase of A, the qualified index increased significantly. When B was at the central level (4 kPa), with the increase of C,

the eligibility index did not change significantly. With the increase of A, the eligibility index increased first and then decreased. When A was at the central level (5.8 mm), the conformity index increased first and then decreased with the increase of B, and the increase of C had little effect on the conformity index.

It can be seen from the influence of each interaction factor of soybean on the qualified index that when C was at the central level (22 r/min), the qualified index increased first and then decreased with the increase of B, and with the increase of A, the qualified index increased significantly. When B was at the central level (4 kPa), the qualification index decreased with the increase of C and increased with the increase of A; when A was at the central level (5.8 mm), the conformity index gradually decreased with the increase of C and B.

4.2. Parameter Optimization

The optimization software of Design-Expert software was used to optimize the analysis, and the best working parameters were obtained: for sowing corn, when the air suction hole diameter was 5.9 mm, the air pressure intensity was 3.5 kPa, and the rotation speed of the seeding plate was 23.8 r/min, the seeding performance was the best. At this time, the seeding qualified index was 95.35%, the reseeding index was 1.45%, and the missed seeding index was 3.23%. For sowing soybean, when the air suction hole diameter was 6.1 mm, the air pressure intensity was 3.5 kPa, and the rotation speed of the seeding plate was 24 r/min, the seeding performance was the best. At this time, the seeding qualified index was 95.76%, the replay index was 3.47%, and the missed seeding index was 0.77%.

4.3. Bench Test and Comparative Test

The test materials were selected from the common maize varieties without appearance damage in the Jilin area, such as *Xianyu 335*, *Zhengdan 958*, and *Hongbo 319*, and the soybean varieties were *Heihe 43*, *Jiyu 99*, and *Jiyu 302*. In this paper, three kinds of corn seeds and three kinds of soybean seeds were evenly mixed to test the performance of the seed-metering device. At the same time, to ensure the seeding performance, the seeding performance test was carried out by installing the seed guide tube.

The bench test of the seed-metering device was carried out in laboratory of the engineering experimental base of Jilin Agricultural University. The JPS-12 type seed-metering device test bench was used to test the universal corn-soybean precision seed-metering device.

The test was carried out by using the trial-produced corn-ordinary steel. To observe the working conditions of the seed-metering device, the black opaque cover was not installed. The effect of the seed-metering device installed on the bench is shown in Figure 20.

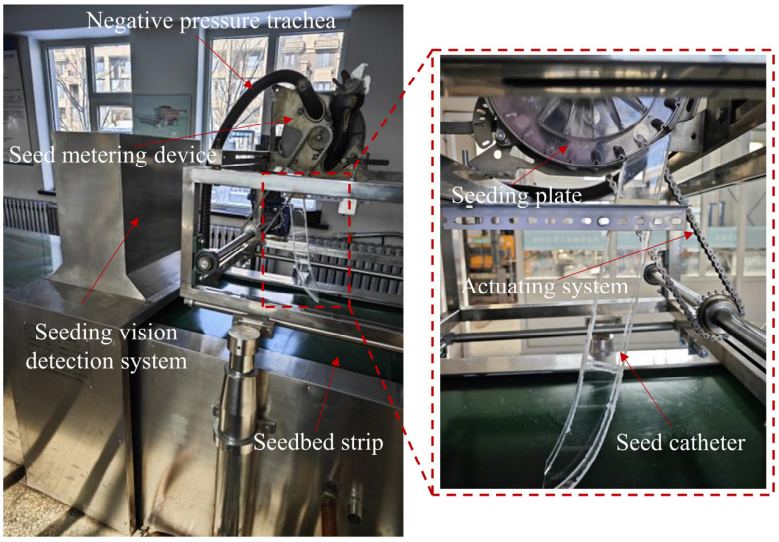

Figure 20. Installation diagram of the seed-metering device.

The bench test was carried out with the optimal working conditions as the test parameters and compared with the traditional soybean plane vertical-disc air-suction seeding-metering device and the air-suction corn precision seed-metering device. The test was repeated five times, and the test results are shown in Table 5. The results showed that the qualified index (average value) of the corn seed test was 95.58%, the replay index (average value) was 1.43%, and the missed sowing index (average value) was 2.99%. The qualified index (average value) of the soybean seed test was 95.74%, the reseeding index (average value) was 3.21%, and the missed sowing index (average value) was 1.05%. The test results were consistent with the optimization results. Because the seed-metering device in this study took into account both corn and soybean seeds, the qualified indexes of the two seeds were slightly smaller than those of the traditional corn and soybean seed-metering device.

Table 5. Comparative test results of corn and soybean.

Level	Corn			Soybean			Corn (Trad)	Soybean (Trad)
	Acceptance Index (%)	Replay Index (%)	Leakage Index (%)	Acceptance Index (%)	Replay Index (%)	Leakage Index (%)	Acceptance Index (%)	Acceptance Index(%)
1	96.12	1.76	2.12	95.56	3.33	1.11	97.63	98.21
2	95.45	1.45	3.1	95.68	3.26	1.06	98.85	98.36
3	95.77	1.32	2.91	95.78	3.25	0.97	97.48	97.89
4	95.21	1.26	3.53	95.64	3.21	1.15	98.53	97.75
5	95.35	1.34	3.31	96.13	2.92	0.95	98.44	98.13
Average	95.58	1.43	2.99	95.74	3.21	1.05	98.2	98.1

The seeding test was carried out under the optimal working conditions of the seed-metering device, and the seeding performance after the seed guide tube was installed in the seed-metering device was detected. The variation coefficient of the seed spacing was used as the evaluation index, and the average value was repeated five times. The variation coefficient of the corn seed spacing was 10.23%, and the variation coefficient of the soybean seed spacing was 9.84%. The two kinds of seed implantation are shown in Figure 21.

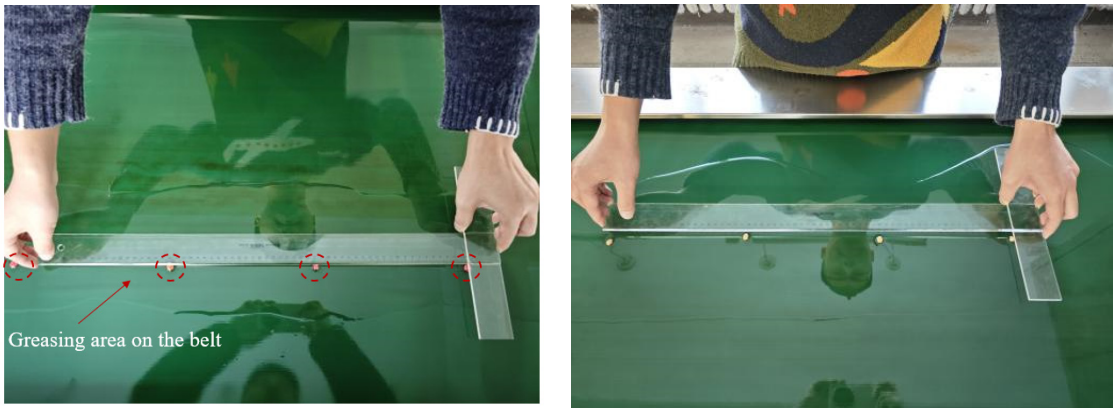

(**a**) (**b**)

Figure 21. Pictures after the completion of planting. (**a**) Corn planting map; (**b**) soybean implantation map.

5. Conclusions

Based on the pneumatic metering device, a universal metering device was designed in this paper. By changing the hole size of the seeding plate, the versatility of corn and soybean seeds was realized. The main research conclusions were drawn as follows:

(1) Through the single-factor and three-factor five-level coupling simulation tests, it was proved that the air suction hole diameter, the air pressure intensity, and the rotation speed of the seeding plate had significant effects on the sowing performance. With the

increase of the air pressure intensity, the air suction hole diameter, and the rotation speed of the seeding plate, the sowing qualified indexes of maize and soybean showed a trend of increasing first and then decreasing. The optimal working parameters for sowing corn were as follows: the air suction hole diameter was 5.9 mm, the air pressure intensity was 3.5 kPa, and the rotation speed of the seeding plate was 23.8 r/min. The optimum working parameters for sowing soybeans were as follows: the air suction hole diameter was 6.1 mm, the air pressure intensity was 3.5 kPa, and the rotation speed of the seeding plate was 24 r/min. Under the optimum working parameters of the seed-metering device, the qualified indexes of corn and soybean seeds were not less than 95%, the reseeding indexes were less than 5%, and the missing indexes were less than 5%, which met the seeding requirements. The results showed that the metering device had good seeding performance and versatility.

(2) The bench verification test was carried out on the optimal working parameters of corn and soybean. The bench test results were not much different from the coupling simulation test results, which proved that the seeding performance of the seed-metering device was consistent with the optimization results.

(3) Through the comparison test with the traditional soybean plane vertical-disc air-suction seed-metering device and the air-suction corn precision seed-metering device, it was found that the qualified indexes of the corn and soybean universal seed-metering device were slightly lower than the qualified indexes of the traditional corn and soybean air-suction seed-metering device, but it still met the requirements of the 'JB/T 51017-1999 [35] precision seeder product quality classification' and the industry standard 'JB/T10293-2013 [36] single grain (precision) seeder technical conditions on the performance of the seed-metering device.

(4) The sowing tests of corn and soybean seeds were carried out under the optimum working parameters of the seed-metering device. In the case of installing the seed guide tube, the coefficients of variation of the grain spacing of corn and soybean seeds were 10.23% and 9.84%, respectively.

(5) In the next research work, the seed particle size distribution will be studied, and the seed group model will be established, so that the simulation process can better predict the seeding effect of the seed-metering device; at the same time, further research will be carried out on the contact between seeds and soil during the seeding process; finally, the corn and soybean universal planter will be studied.

Author Contributions: Conceptualization, X.J., D.H. and J.Z.; methodology, J.Z.; software, L.F.; validation, X.J. and D.H.; investigation, X.J. and S.L.; resources, D.H. and X.J; visualization, L.F.; writing—original draft preparation, J.Z.; funding acquisition, X.J. and D.H. All authors have read and agreed to the published version of the manuscript.

Funding: This research was financially supported by the Science and Technology Development Plan Project of Jilin Province (No. 20200402008NC) and the National Key Research and Development Program (grant number: 2023YFD1500404).

Data Availability Statement: Data are contained within the article.

Conflicts of Interest: The authors declare no conflict of interest.

References

1. Food and Agriculture Organization. *World Food and Agriculture Statistical Yearbook*; FAO: Roma, Italy, 2023.
2. Yang, W.; Nigonb, T.; Hao, Z.; Paiao, G.D.; Fernández, F.G.; Mulla, D.; Yang, C. Estimation of corn yield based on hyperspectral imagery and convolutional neural network. *Comput. Electron. Agric.* **2021**, *184*, 106092. [CrossRef]
3. Di Salvo, J.; Lee, C.; Salmerón, M. Regional multi-environment analysis of corn productivity and yield stability as impacted by hybrid maturity. *Field Crop. Res.* **2021**, *262*, 108025. [CrossRef]
4. Yang, L.; He, X.T.; Cui, T.; Zhang, D.X. Development of mechatronic driving system for seed meters equipped on conventional precision corn planter. *Int. J. Agric. Biol. Eng.* **2015**, *8*, 1–9.
5. Santa Ormond, A.T.; Angeli Furlani, C.E.; De Oliveira, M.F.; De Freitas Noronha, R.H.; de Oliveira Tavares, T.; De Menezes, P.C. Maize Sowing Speeds and Seed-Metering Mechanisms. *J. Agric. Sci.* **2018**, *10*, 468.

6. Jia, H.L.; Chen, Y.L.; Zhao, J.L.; Guo, M.Z.; Huang, D.Y.; Zhuang, J. Design and key parameter optimization of an agitated soybean seed metering device with horizontal seed filling. *Int. J. Agric. Biol. Eng.* **2018**, *11*, 76–87. [CrossRef]
7. Liao, Y.T.; Wang, L.; Liao, Q.X. Design and test of an inside-filling pneumatic precision centralized seed-metering device for rapeseed. *Int. J. Agric. Biol. Eng.* **2017**, *10*, 56–62.
8. Liu, H.; Liu, J.; Tang, S.; Xu, X. Design on opposed inclined-plate high-speed precision seed-metering device and its working mechanism analysis. *Trans. Chin. Soc. Agric. Eng.* **2016**, *32*, 24–31.
9. Kamgar, S.; Noei-Khodabadi, F.; Shafaei, S.M. Design, development and field assessment of a controlled seed metering unit to be used in grain drills for direct seeding of wheat. *Inf. Process. Agric.* **2015**, *2*, 169–176. [CrossRef]
10. Zhai, J.B.; Xiao, J.F.; Zhou, Y.; Zhang, S. Design and experimental study of the control system for precision seed-metering device. *Int. J. Agric. Biol. Eng.* **2014**, *7*, 13–18.
11. Tang, H.; Xu, F.D.; Xu, C.S.; Zhao, J.L.; Wang, Y.J. The influence of a seed drop tube of the inside-filling air-blowing precision seed-metering device on seeding quality. *Comput. Electron. Agric.* **2023**, *204*, 107555. [CrossRef]
12. Zhong, W.D.; Zhao, X.; Liu, F.; Bai, H.B.; Dong, W.X.; Hu, H.T.; Kong, X. Design and Experiment of Precision Seed Metering Device for Flow Adsorption of Quinoa Seeds. *Agriculture* **2024**, *14*, 434. [CrossRef]
13. Hu, M.J.; Xia, J.F.; Zhou, M.K.; Liu, Z.Y.; Xie, D.Y. Design and Experiment of Seed-Cleaning Mechanism for Inside-Filling Pneumatic Cotton Precision Seed-Metering Device. *Agriculture* **2022**, *12*, 1217. [CrossRef]
14. Tang, H.; Xu, F.D.; Guan, T.Y.; Xu, C.S.; Wang, J.W. Design and test of a pneumatic type of high-speed maize precision seed metering device. *Comput. Electron. Agric.* **2023**, *211*, 107997. [CrossRef]
15. Wang, J.; Tang, H.; Wang, J.; Xin, L.; Huang, H. Optimization design and experiment on ripple surface type pickup finger of precision maize seed metering device. *Int. J. Agric. Biol. Eng.* **2017**, *10*, 61–71.
16. Liu, J.; Cui, T.; Zhang, D.; Huang, S.; Shi, S. Experimental study on pressure of air blowing precision seed-metering device. *Trans. Chin. Soc. Agric. Eng.* **2011**, *27*, 18–22.
17. Liao, Q.; Yang, B.; Li, X.; Liao, Y.; Zhang, N. Simulation and experiment of insidefilling air-blow precision metering device for rapeseed. *Trans. Chin. Soc. Agric. Mach.* **2012**, *43*, 51–54.
18. Yu, J.; Wang, G.; Xin, N.; Fu, H. Simulation analysis of working process and performance of cell wheel metering device. *Trans. Chin. Soc. Agric. Mach.* **2011**, *42*, 83–87, 101.
19. Wu, Z.; Li, M.; Lei, X.; Wu, Z.; Jiang, C.; Zhou, L.; Ma, R.; Chen, Y. Simulation and parameter optimisation of a centrifugal rice seeding spreader for a UAV. *Biosyst. Eng.* **2020**, *192*, 275–293. [CrossRef]
20. Xi, X.; Gao, W.; Gu, C.; Shi, Y.; Han, L.; Zhang, Y.; Zhang, B.; Zhang, R. Optimisation of no-tube seeding and its application in rice planting. *Biosyst. Eng.* **2021**, *210*, 115–128. [CrossRef]
21. Hu, M.J.; Xia, J.F.; Zhou, M.K.; Liu, Z.Y.; Xie, D.Y. Design and Experiment of Inside-filling Pneumatic High Speed Precision Seed-metering Device for Cotton. *Trans. Chin. Soc. Agric. Mach.* **2021**, *52*, 73–85.
22. Shah, K.; Alam, M.S.; Nasir, F.E.; Qadir, M.U.; Haq, I.U. Design and Performance Evaluation of a Novel Variable Rate Multi-Crop Seed Metering Unit for Precision Agriculture. *IEEE Access* **2022**, *10*, 133152–133163. [CrossRef]
23. Wang, D.W.; Ji, R.Q.; He, X.N. Study of a high-speed precision seed discharger for peanuts with drive-guide combination slot-assisted seed attachment and air suction. *J. Agric. Mech.* **2023**, *54*, 59–70+149.
24. Shi, S.B.; Zheng, Y.N.; Yang, N. Simulation analysis of seed guiding process of air-absorbing duckbill type corn precision seed discharger. *Agric. Mech. Res.* **2023**, *45*, 24–29.
25. Liu, R.; Liu, Z.J.; Liu, L.J. Design and testing of a high-speed air-aspirated seed discharger for disturbance-assisted seed filling of corn. *J. Agric. Mech.* **2022**, *53*, 50–59.
26. Ding, L.; Yang, L.; Zhang, D.X. Parametric design and test of seed cleaning mechanism of air-absorbing corn seed discharger. *Trans. Chin. Soc. Agric. Mach.* **2019**, *50*, 47–56.
27. Jia, H.L.; Chen, Y.L.; Zhao, J.L. Design and test of pneumatic-absorption-mechanical compound soybean precision seeder. *J. Agric. Mech.* **2018**, *49*, 75–86+139.
28. Karayel, Z.D.; Barut, B.; Özmerzi, A. Mathematical Modelling of Vacuum Pressure on a Precision Seeder. *Biosyst. Eng.* **2004**, *87*, 437–444. [CrossRef]
29. He, S.Y.; Zang, Y.; Huang, Z.S.; Tao, W.Y.; Xing, H.; Qin, W.; Jiang, Y.C.; Wang, Z.M. Design of and Experiment on a Cleaning Mechanism of the Pneumatic Single Seed Metering Device for Coated Hybrid Rice. *Agriculture* **2022**, *12*, 1239. [CrossRef]
30. Gaikwad, B.B.; Sirohi, N.P.S. Design of a low-cost pneumatic seeder for nursery plug trays. *Biosyst. Eng.* **2008**, *99*, 322–329. [CrossRef]
31. Zhao, Z.; Li, Y.; Chen, J.; Xu, L. Numerical analysis and laboratory testing of seed spacing uniformity performance for vacuum-cylinder precision seeder. *Biosyst. Eng.* **2010**, *106*, 344–351.
32. Onal, I.; Degirmencioglu, A.; Yazgi, A. An evaluation of seed spacing accuracy of a vacuum type precision metering unit based on theoretical considerations and experiments. *Turk. J. Agric. For.* **2012**, *36*, 133–144.
33. Yasir, S.H.; Liao, Q.; Yu, J.; He, D. Design and test of a pneumatic precision metering device for wheat. *Agric. Eng.* **2012**, *14*, 16–25.
34. Ding, Y.; Liao, Q.; Huang, H. The seeding migration trajectory extraction and analysis of pneumatic precision metering device for rapeseed. *J. Food. Agric. Environ.* **2013**, *11*, 477–482.

35. *JB/T 51017-1999*; Product Quality Grading of Precision Seeder for Intertillage Crops. MIIT: Beijing, China, 1999.
36. *JB/T 10293-2013*; Technical Conditions of Single Grain (Precision) Seeder. MIIT: Beijing, China, 2013.

Disclaimer/Publisher's Note: The statements, opinions and data contained in all publications are solely those of the individual author(s) and contributor(s) and not of MDPI and/or the editor(s). MDPI and/or the editor(s) disclaim responsibility for any injury to people or property resulting from any ideas, methods, instructions or products referred to in the content.